Applied and Environmental Microbiology, Aug. 2005, p. 4414–4426 Vol. 71, No. 8
0099-2240/05/$08.00+0 doi:10.1128/AEM.71.8.4414–4426.2005

Shewanella oneidensis MR-1 Uses Overlapping Pathways for Iron Reduction at a Distance and by Direct Contact under Conditions Relevant for Biofilms

Douglas P. Lies,[1]† Maria E. Hernandez,[2]† Andreas Kappler,[1] Randall E. Mielke,[3] Jeffrey A. Gralnick,[1] and Dianne K. Newman[1,2]*

Department of Geological and Planetary Sciences[1] and Department of Environmental Science & Engineering,[2] California Institute of Technology, Pasadena, California 91125, and Jet Propulsion Laboratory, Pasadena, California[3]

Received 27 May 2004/Accepted 20 February 2005

We developed a new method to measure iron reduction at a distance based on depositing Fe(III) (hydr)oxide within nanoporous glass beads. In this "Fe-bead" system, *Shewanella oneidensis* reduces at least 86.5% of the iron in the absence of direct contact. Biofilm formation accompanies Fe-bead reduction and is observable both macro- and microscopically. Fe-bead reduction is catalyzed by live cells adapted to anaerobic conditions, and maximal reduction rates require sustained protein synthesis. The amount of reactive ferric iron in the Fe-bead system is available in excess such that the rate of Fe-bead reduction is directly proportional to cell density; i.e., it is diffusion limited. Addition of either lysates prepared from anaerobic cells or exogenous electron shuttles stimulates Fe-bead reduction by *S. oneidensis*, but iron chelators or additional Fe(II) do not. Neither dissolved Fe(III) nor electron shuttling activity was detected in culture supernatants, implying that the mediator is retained within the biofilm matrix. Strains with mutations in *omcB* or *mtrB* show about 50% of the wild-type levels of reduction, while a *cymA* mutant shows less than 20% of the wild-type levels of reduction and a *menF* mutant shows insignificant reduction. The Fe-bead reduction defect of the *menF* mutant can be restored by addition of menaquinone, but menaquinone itself cannot stimulate Fe-bead reduction. Because the *menF* gene encodes the first committed step of menaquinone biosynthesis, no intermediates of the menaquinone biosynthetic pathway are used as diffusible mediators by this organism to promote iron reduction at a distance. CymA and menaquinone are required for both direct and indirect mineral reduction, whereas MtrB and OmcB contribute to but are not absolutely required for iron reduction at a distance.

Microbial iron(III) reduction plays an important role in a variety of biogeochemical cycles (29, 44), and it is a promising system for bioremediation of organic and metal contaminants (27), corrosion control (14), and harvesting electrical current from marine sediments (6). To better predict and/or stimulate the activity of iron-reducing organisms in the environment, it is essential to be able to quantify these organims, as well as to understand the mechanisms by which any given microbial community catalyzes iron reduction.

Many studies have been performed to assess the distribution of metal-reducing organisms in the environment (11, 28), as well as to determine the mechanistic basis of iron reduction, both with respect to what enables it (12) and what constrains it (21, 51). *Geobacter* (11, 30, 32, 60), *Geothrix* (10, 46), and *Shewanella* (8, 19, 40, 66, 70) species have been the primary objects of investigation in these studies. These organisms are found in different environments and are generally thought to reduce iron oxides by different mechanisms in response to different environmental conditions. For example, when nutrients are sparse, both *Shewanella* and *Geobacter* are believed to reduce iron oxides through direct electron transfer between outer membrane proteins and the oxide surface (17, 45). In situations where nutrients are more abundant and/or the cells grow in biofilms, it has been suggested that iron reduction proceeds through the cycling of mediators (such as ferric iron chelators or extracellular electron shuttles) that enable the bacteria to reduce the metal oxides at a distance (25, 47, 53). Recently, it has even been suggested that ferrous iron itself might be sufficient to catalyze the reductive dissolution of ferric oxides, liberating sufficient dissolved ferric iron to sustain microbial respiration (20).

Several years ago, our group suggested that a menaquinone-like compound might play a role in extracellular electron transfer from *Shewanella oneidensis* MR-1 to iron oxides (48). This suggestion was based on the following facts: (i) a mutant of MR-1 defective in the *menC* gene (open reading frame [ORF] SO4575 in the MR-1 genome sequence [22] that encodes *o*-succinylbenzoic acid synthase, which is required for menaquinone biosynthesis) could be rescued with respect to its ability to reduce 2,6-anthraquinone disulfonate (AQDS) by an extracellular diffusible factor released by the wild type; (ii) the *menC* mutant does not make this factor under any conditions; and (iii) semipurified fractions of culture fluids from the wild type with maximal activity for stimulation of AQDS reduction by the *menC* mutant have spectrophotometric properties reminiscent of those of quinones. However, as stated in the conclusion to that study, it was not clear at the time whether the observed rescue of the *menC* mutant was simply due to the restoration of menaquinone biosynthesis by cross-feeding of a

* Corresponding author. Mailing address: Department of Geological and Planetary Sciences, Caltech, Pasadena, CA 91125. Phone: (626) 395-6790. Fax: (626) 683-0621. E-mail: dkn@gps.caltech.edu.
† D.P.L. and M.E.H. contributed equally to this work.

menaquinone precursor or due to the provision of an extracellular electron shuttle that was required for electron transfer to AQDS. Moreover, we did not demonstrate in that work that the excreted factor could shuttle electrons to Fe(III) minerals.

Although we (23) and other workers (36) subsequently determined that restoration of menaquinone biosynthesis explained the phenotype that led us to hypothesize that *S. oneidensis* produces extracellular electron shuttles that catalyze mineral reduction, Nevin and Lovley demonstrated that the general concept was correct for different strains. These authors reported evidence for indirect Fe(III) reduction by *Shewanella algae* strain BrY (47) and *Geothrix fermentans* (46) but not by *Geobacter metallireducens* using an iron-containing alginate bead system (45). Although no electron shuttling molecules were isolated in these studies, in the case of *G. fermentans* preliminary thin-layer chromatograms of culture filtrates suggested the presence of a hydrophilic quinone(s) (46); additional data that supported the presence of Fe(III)-chelating molecules as mediators of iron reduction at a distance were also provided (47). More recently, iron reduction was demonstrated to occur at a distance in iron-reducing enrichment cultures, but neither the nature of the mediator nor the organism(s) involved was determined (61). In a few cases, specific molecules have been identified as extracellular electron shuttles to minerals; these molecules include cell-associated melanin (63, 64) and phenazines and other redox-active antibiotics (24).

Whether *S. oneidensis* strain MR-1 itself reduces iron oxides at a distance has never been directly demonstrated, and the capacity of strain MR-1 for this process has been called into question (36). Because this strain is an important model system in geomicrobiology, we set out to determine whether in fact it could perform iron reduction at a distance. In our hands, the alginate bead method of Nevin and Lovley (47) yielded ambiguous results, so we developed a new method to test for this phenotype. Here we describe how we used this method to answer whether strain MR-1 reduces iron at a distance and, if it does, under what conditions and through which pathway(s) it does so.

MATERIALS AND METHODS

Bacterial strains, culture conditions, and chemicals. *S. oneidensis* MR-1 was originally isolated from Oneida Lake in New York (40). It was grown in either Luria-Broth (LB) medium (34), a minimal medium (pH 7.2) (55), or LM-lactate (LML) medium (37) at 30°C. The *omcB* mutant DKN247, with a mutation in ORF SO1778 of the *S. oneidensis* MR-1 genome sequence (22), and the *mtrB* mutant DKN248, with a mutation in ORF SO1776, were isolated during screening for mutants of MR-1 defective in Fe(III) (hydr)oxide reduction using Tn*phoA′*-1 for mutagenesis as described previously (57). The *menF* mutant DKN249, with a mutation in ORF SO4713, and the *cymA* mutant DKN250, with a mutation in ORF SO4591, were isolated during screening for mutants of MR-1 defective in reduction of Fe(III) (hydr)oxide-coated porous glass beads (Fe-beads) using Tn*phoA′*-1. The locations of the transposon insertions in these mutants were determined by arbitrary PCR sequencing (49) and were confirmed by PCR amplification using gene-specific primers to amplify the regions containing the insertions or using a combination of gene-specific and transposon-specific primers.

Other strains used in this study were *Shewanella algae* BrY (8), *Shewanella putrefaciens* CN-32 (70), *Shewanella* sp. strain ANA-3 (55), and *Escherichia coli* MG1655 (5), and these organisms were cultured under the same conditions. The complex organic chemicals menaquinone MK-4 (vitamin K_2) and AQDS were purchased from Sigma. Phenazine methosulfate (PMS) was purchased from Fluka. 1,4-Dihydroxy-2-naphthoic acid (DHNA) was purchased from Aldrich.

Synthesis of Fe-beads. Fe-beads were prepared by adding 25 g porous glass beads (native CPG-500 beads from Prime Synthesis Inc., Aston, PA; particle size, ~100 μm; surface area, 108 m^2/g; pore volume, 1.4 ml/g; average pore size, 50 nm; bulk density, 0.29 g/ml) to 500 ml of a 50 mM $FeCl_3$ solution in a 2-liter Erlenmeyer flask. Poorly crystalline ferric (hydr)oxide [Fe(III) (hydr)oxide] was precipitated on the inner and outer glass bead surfaces by dropwise addition of 2 M KOH in small portions within several hours (the flask was shaken by hand while the KOH was added). After the pH reached 6.5 to 7, the suspension was allowed to equilibrate for several hours before the pH was readjusted to pH 7. Excess Fe(III) (hydr)oxide was decanted after gentle shaking [the coated glass beads were slightly heavier than the excess Fe(III) (hydr)oxide]. The Fe-beads were washed 10 times with 50 mM KCl and five times with H_2O, collected with a paper filter, and freeze-dried or air dried before storage at room temperature. The Fe(III) (hydr)oxide produced during this procedure was identified by X-ray diffraction of excess Fe(III) precipitates isolated from the supernatant. X-ray diffraction spectra were obtained with a Scintag Pad V X-ray powder diffractometer using Cu-Kα radiation operating at 35 kV and 30 mA and a θ-2θ goniometer equipped with a germanium solid-state detector. For each scan we used a 0.04° step size from 10° to 80° with a counting time of 2 s per step.

SEM. For scanning electron microscopy (SEM) Fe-beads (~50 mg) were fixed on double-sticking carbon tape mounted on a sample holder and coated with a few-nanometer-thick layer of carbon using a carbon evaporator (Edwards E306A; Edwards, United Kingdom). The samples were examined with a LEO 1550VP field emission scanning electron microscope equipped with an Oxford INCA energy-dispersive X-ray spectrophotometer. The system was operated at 1 to 15 kV for high-resolution secondary electron imaging and elemental analysis.

Environmental scanning electron microscopy. Whole-mount samples were imaged using an FEI EM-30 microscope at 20 kV with a 10.7-mm working distance. The stage temperature was maintained at 4°C with an environmental chamber pressure of 4.5 torr to achieve an internal relative humidity of 85 to 90%.

TEM and EDS. For transmission electron microscopy (TEM) and energy-dispersive X-ray spectroscopy (EDS), for each sample a volume of culture was fixed with 2% (vol/vol) glutaraldehyde and kept at 4°C until it was embedded. Fixed cultures were washed three times in water by centrifugation, and the final pellets were dispersed in Noble agar. One half of each sample was stained with 2% osmium tetroxide and 2% uranyl acetate (1 h each), while the other half was left unstained. Both stained and unstained specimens were subjected to ethanol dehydration (25% ethanol, 50% ethanol, 75% ethanol, and 100% ethanol [twice], 15 min each), followed by 15-min washes with 50:50 ethanol:acetone and 100% acetone before incubation in 50:50 acetone:Epon resin overnight. Samples were embedded in 100% Epon resin and dried for 24 h at 60°C, after which they were sectioned (60 nm) with an MT-X ultramicrotome with a 55° Diatome diamond knife. Ultrathin sections were placed on 200-mesh copper grids with a Formvar/carbon coating. The prestained ultrathin section samples were subsequently poststained with 2% uranyl acetate before final imaging. Thin sections were examined with an Akashi EM-002B LaB_6 transmission electron microscope operating at 100 kV and equipped with an Oxford EDS unit. The selected area sampled by the Oxford spectrum analyzer was approximately 500 to 300 nm in diameter. The acquisition rates were maintained at 10 to 20% dead time with 60 s of live time at 83 kV. The electron beam was defocused at the condenser lens to maintain counting rates of 1 to 2 kcps.

Confocal microscopy. Samples were fixed with 2% glutaraldehyde and stained with the Live-Dead dye (L-7012; Molecular Probes) as a convenient general stain for imaging with an inverted Zeiss LSM 510 confocal microscope with a 40× water immersion lens at the Biological Imaging Center at Caltech. All cells and the beads were visualized using laser excitation at 543 nm and an LP560 emission filter.

Fe-bead reduction assays. MR-1 and other strains were initially grown under oxygen-limited conditions in LB medium (10 ml in 18-mm test tubes incubated aerobically with shaking at 30°C), harvested in the early stationary phase (optical density at 600 nm [OD_{600}] = 2 to 3), and then washed three times with LML medium. The washed cells were diluted to an OD_{600} of 0.1 in LML medium with 1 mM fumarate as an electron acceptor and preincubated for 4 to 5 h at 30°C in a Coy anaerobic chamber ($N_2/CO_2/H_2$ [80:15:5] atmosphere). For *E. coli*, the anaerobic preincubation was performed with LM medium with 0.5% glycerol and 1 mM fumarate. In experiments in which menaquinone MK-4 was added to rescue anaerobic respiration in the *menF* mutant, 10 μM MK-4 in ethanol was added during the anaerobic preincubation with fumarate. The cells were then washed three times in the anaerobic chamber with minimal medium, inoculated with Fe-glass beads (0.02 g) or freshly prepared Fe(III) (hydr)oxide mineral (final concentration, 1 mM) in 3 ml of minimal medium, and incubated in capped tubes without shaking at 30°C in the anaerobic chamber. The initial cell density

used in the experiments was 6.7×10^8 cells/ml unless indicated otherwise. Incubation was stopped after 3 days by addition of 0.75 ml of 12 N HCl to extract the total amount of iron present in the tubes. The Fe(II) in the acidified culture samples was quantified by the ferrozine assay (59), and the total iron [Fe(II) plus Fe(III)] was quantified after a reduction step with hydroxylamine hydrochloride ($NH_2OH \cdot HCl$) (31). Killed cells were prepared by exposing cells to 20% formaldehyde for 1 h, after which the cells were washed in minimal medium prior to incubation in the Fe-bead assay. Supernatants from Fe-bead reduction experiments were prepared from high-cell-density tubes (6.7×10^8 cells/ml) in which at least 80% of the measurable iron was reduced, and they were vortexed and centrifuged either in the anaerobic chamber to produce reduced supernatants or aerobically to produce oxidized supernatants. For experiments with supernatant additions, supernatants were processed and then added as 66% of the final volume without a filtration step (to avoid losing organic molecules by adsorption to the filter) to new tubes containing Fe-beads and cells at a final density of 1×10^8 cells/ml. "Aerobic cell" lysates were prepared by concentrating 10 ml of an aerobic LB medium-grown stationary phase culture in 1 ml HEPES buffer (pH 7.2), sonicating the preparation with 10-s pulses for 1 min (five cycles on ice), and centrifuging the preparation to remove the unlysed cells; 200 μl was added to 3-ml Fe-bead tubes. "Anaerobic cell" lysates were prepared with 2×10^{10} cells that were used as the inoculum for the Fe-bead system in 1 ml of minimal medium. These cells were sonicated and centrifuged as described above for the "aerobic cell" lysates and added as shown in Table 2. For experiments in which shuttles or chelators were added, the Fe-bead cultures were sampled daily during 3 days of incubation. Reduction rates were determined as the slopes and standard errors for the 24- to 72-h samples using the LINEST function in Excel. For experiments in which Fe(II) was added, the Fe(II) stock solutions were made from ferrous ammonium sulfate stored in the Coy anaerobic chamber and added to anaerobic water.

Comparison of aerobically and anaerobically grown inocula. Aerobically grown cells of strain MR-1 were prepared by inoculating 25 μl of an aerobic overnight culture grown in LB medium into 25 ml of LB medium in a 250-ml Erlenmeyer flask and incubating this culture aerobically with shaking at 250 rpm at 30°C until the OD_{600} reached 0.05 to 0.1. The cells were harvested by centrifugation, washed three times with LML medium, and then diluted into 250 ml of LML medium in a 2-liter Erlenmeyer flask and incubated aerobically with shaking at 250 rpm at 30°C until the OD_{600} reached 0.07 to 0.1. The cells were then harvested, washed, and incubated with Fe-glass beads as described above, using 6.7×10^8 cells/ml. Anaerobically grown cells were prepared by inoculating 500 μl of oxygen-limited cells prepared as described above for the typical Fe-bead experiment into 250 ml of LML medium containing 10 mM fumarate as an electron acceptor. This culture was incubated at 30°C in the Coy anaerobic chamber until the OD_{600} reached 0.1. The cells were then harvested, washed, and incubated with Fe-beads as described above. When necessary, chloramphenicol was added to the Fe-bead system at a final concentration of 105 μg/ml from a 30-mg/ml stock solution in ethanol to inhibit further protein synthesis.

Protein quantification. To determine total protein levels during Fe-bead reduction, the acidified Fe-bead cultures used for the iron reduction determinations were incubated at 37°C for 30 min and then vortexed for 30 s. Samples (1.8 ml) of the supernatants were mixed with 75 μl of 10 M trichloroacetic acid and incubated for 30 min on ice. The samples were centrifuged for 15 min at 4°C, the supernatant was removed, and the pellet was resuspended in 500 μl of 0.1 N NaOH and boiled for 5 min. Protein was measured using a commercially available version of the Bradford assay (Bio-Rad) with bovine serum albumin as the standard.

Quantification of soluble and mineral Fe(III) reduction and AQDS reduction by mutant strains. Strains used for Fe(III) reduction assays were inoculated in duplicate from single colonies and grown overnight in LB medium with vigorous shaking at 30°C. Two microliter from each overnight culture was used to inoculate 198 μl of minimal medium containing 10 mM lactate and 1 mM ferric citrate or 0.5 mM amorphous Fe(III) (hydr)oxide in microtiter plate wells. Plates were transferred into the Coy anaerobic chamber and incubated at 30°C. Samples were transferred to a new microtiter plate at various times and removed from the anaerobic chamber. These samples were immediately acidified, and Fe(II) was quantified as described above.

For AQDS reduction assays, strains were inoculated in triplicate and were grown to an OD_{600} of 2.0 to 2.5 under oxygen-limited conditions as described above for the Fe-bead cultures. The cells were washed in the Coy anaerobic chamber with anaerobic minimal medium and then diluted to an OD_{600} of 0.2 into 2.5 ml of reduction buffer (24) containing 1 mM AQDS, 10 mM HEPES (pH 7.5), 4 mM $MgCl_2$, and 2 mM each of lactate, succinate, and pyruvate in a sealed quartz anaerobic cuvette. The cuvettes were incubated at 30°C and assayed every 15 min for AQDS reduction and cell density by measuring the absorbance at 450 nm and the absorbance at 600 nm, respectively.

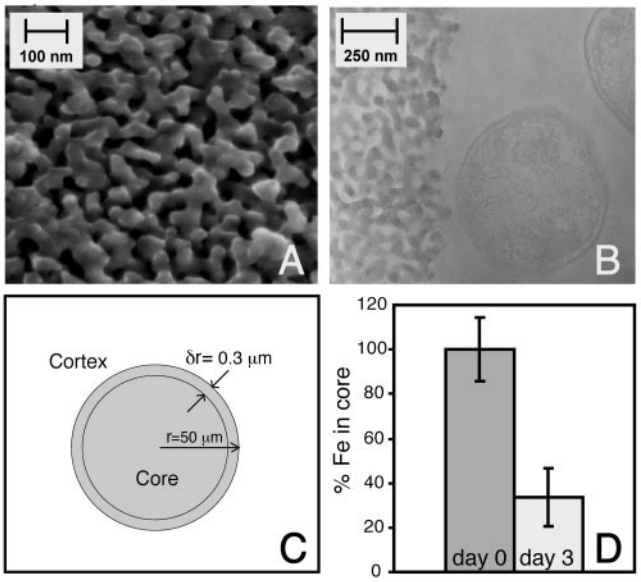

FIG. 1. Fe-bead characterization. (A and B) SEM (A) and TEM (B) images of Fe-beads, showing the surface structure, 50-nm-diameter pores, and the size of the pores relative to an *S. oneidensis* MR-1 cell (on the right side in panel B). (C) Schematic diagram providing the dimensions of the bead core and cortex. (D) Percentages of iron in the core of the beads on days 0 and 3 as determined by TEM and EDS, prior to acid extraction. The error bars indicate the standard deviations for 50 EDS measurements from a single experiment (cell density, 6.7×10^8 cell/ml).

RESULTS

Measuring Fe(III) reduction at a distance by *S. oneidensis* MR-1 using Fe-beads. We synthesized Fe(III) (hydr)oxide-coated porous glass beads to provide a system with a high surface area, small pores, and a chemically stable and inert inorganic support matrix to test for iron reduction at a distance. Analysis of the surface of the Fe-beads by SEM (Fig. 1A) revealed that the Fe(III) (hydr)oxide-coated glass beads looked very similar to the glass beads before mineral precipitation. We could not distinguish Fe(III) (hydr)oxide particles on the surface of the Fe-beads, except for one electron micrograph in which an iron aggregate was found in a depression on the Fe-bead surface. TEM demonstrated that interconnected pores with an average diameter of 50 nm comprised the bulk of the Fe-beads' interior, and the diameter of a typical MR-1 cell was about 10 times the diameter of these pores (Fig. 1B). Because the glass beads had a very large surface area (108 m^2/g), it is likely that during mineral precipitation, Fe(III) was adsorbed at multiple sites and that the growth of Fe(III) (hydr)oxide crystals from each of the seeds was limited and therefore not distinguishable by the forms of microscopy that we used.

Although the Fe(III) (hydr)oxide coating around the pores cannot be seen in the SEM and TEM images, EDS of thin sections of the Fe-beads in randomly selected 0.3-μm-diameter circular areas showed that iron was homogeneously distributed

throughout the matrix, whereas no iron was detected in the original glass bead matrix. To determine the amount of the Fe(III) (hydr)oxide present within the bead matrix (i.e., the fraction that could not be reduced by direct contact), we defined the cortex of a bead as the 0.3-μm-thick outer layer of the bead and the core as the remainder of the bead volume (Fig. 1C) and determined the iron contents of these regions by EDS. Iron constituted an average of 0.41 atomic% of the core, with a standard deviation ($u\%\mathrm{Fe}_{\mathrm{core}}$) of 0.1 atomic% ($n = 50$), and 1.6 atomic% of the cortex ($\%\mathrm{Fe}_{\mathrm{cortex}}$), with a standard deviation ($u\%\mathrm{Fe}_{\mathrm{cortex}}$) of 0.7 atomic% ($n = 50$); 0.1 atomic% iron was left in the core of the beads after the extraction procedure used to measure iron in our experiments, and therefore the total amount of extractable iron in the core was 0.31 atomic% ($\%\mathrm{Fe}_{\mathrm{core}}$, 0.41 to 0.1). Given these values and assuming a spherical shape for the beads (radius, 50 μm), we calculated the percentage of the total measurable iron that was originally in the cortex ($\mathrm{Fe}_{\%\mathrm{from\_cortex}}$) (equation 1) and the uncertainty of this number ($u\mathrm{Fe}_{\%\mathrm{from\_cortex}}$) (equation 2).

$$\mathrm{Fe}_{\%\ \mathrm{from\_cortex}} = \frac{\%\mathrm{Fe}_{\mathrm{cortex}} V_{\mathrm{cortex}}}{\%\mathrm{Fe}_{\mathrm{cortex}} V_{\mathrm{cortex}} + \%\mathrm{Fe}_{\mathrm{core}} V_{\mathrm{core}}} \times 100\% \quad (1)$$

$$u\mathrm{Fe}_{\%\ \mathrm{from\_cortex}} = \sqrt{\left(\frac{d\mathrm{Fe}_{\%\ \mathrm{from\_cortex}}}{d\%\mathrm{Fe}_{\mathrm{cortex}}} u\%\mathrm{Fe}_{\mathrm{cortex}}\right)^2 + \left(\frac{d\mathrm{Fe}_{\%\ \mathrm{from\_cortex}}}{d\%\mathrm{Fe}_{\mathrm{core}}} u\%\mathrm{Fe}_{\mathrm{core}}\right)^2} \times 100\% \quad (2)$$

where V_{cortex} is the volume of the cortex and V_{core} is the volume of the core. Based on this analysis, we estimated that a maximum of 8.9 ± 4.6% of the total measurable iron in the system was present in the cortex and that at least 86.5% of the measurable iron in the system (considering the average amount of iron in the cortex [8.9%] plus its standard deviation [4.6%]) therefore required reduction by a mechanism that did not involve direct contact.

We next used the Fe-beads to determine whether high-density anaerobically induced cultures of MR-1 could reduce iron at a distance. When anaerobically preincubated MR-1 cells were inoculated at a concentration of 6.7×10^8 cells/ml into minimal medium with 20 mg of the Fe-beads and incubated anaerobically, most of the iron in the system (1.1 mM) was reduced within 3 days. Reduction of the 86.5% of the iron that was within the cortex of the Fe-beads occurred in the absence of direct contact by the cells. This conclusion was supported by TEM images of the beads at the end of the experiments, which showed that the beads maintained their structure and integrity (Fig. 1B), and by EDS analyses, which showed that the iron in the core of the beads was depleted during the reduction process (Fig. 1D). The oxidation state of the iron that remained in the bead core following extraction is not known. Supernatants from high-cell-density Fe-bead cultures contained about 10% dissolved Fe(II), and the rest was presumably bound to the cells, the exopolysaccharide, or the beads or was precipitated as iron minerals. We did not observe dissolved Fe(III) at detectable concentrations (>10 μM) in these cultures.

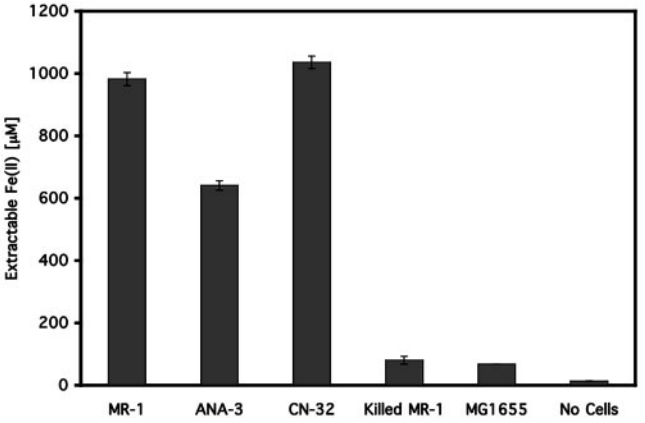

FIG. 2. Reduction of Fe-beads by *Shewanella* strains. The strains used were *S. oneidensis* MR-1, *Shewanella* sp. strain ANA-3, *S. putrefaciens* CN-32, and *E. coli* MG1655. Killed MR-1 cells were killed by formaldehyde treatment as described in Materials and Methods. The data are the averages of duplicate experiments, and the error bars indicate the data ranges for 3-day incubations with Fe-beads.

Other strains of *Shewanella* were also examined for the capacity to reduce iron at a distance using the Fe-beads. When tested under the same conditions that were used for *S. oneidensis* MR-1, *S. putrefaciens* CN-32 and *Shewanella* sp. strain ANA-3 both reduced most of the iron within the Fe-beads, although the amount of iron reduced depended on the strain (Fig. 2). *S. algae* BrY also reduced a considerable portion of the iron within the Fe-beads, but the results were highly variable for this organism due to considerable lysis of the cells during the washing and preincubation steps (data not shown). Strain BrY was previously shown to reduce iron within alginate beads in the system of Nevin and Lovley (47). *E. coli* MG1655 cells reduced less than 10% of the iron in the Fe-beads (Fig. 2); this amount was similar to the amount of iron reduced by formaldehyde-killed cells of *S. oneidensis* MR-1. Because MG1655 prepared under these conditions grew anaerobically with glycerol and fumarate (data not shown) and was therefore metabolically active, this result indicates that reduction of the iron within the core of the Fe-beads was not merely a function of incubation in the presence of bacteria but instead was due to the presence of live *Shewanella* cells in the incubation mixtures. All further experiments were performed using *S. oneidensis* MR-1.

Biofilm formation during Fe-bead reduction. Fe-beads incubated with MR-1 formed clumps in the bottoms of the tubes during incubation that were not dislodged when the tubes were gently inverted (Fig. 3A). Clumping did not occur in tubes without cells or in tubes with killed cells, suggesting that the cells actively formed a biofilm in the presence of the Fe-beads that bound the beads together. Confocal microscopy of stained samples showed that MR-1 cells first attached to the Fe-bead surface and then formed microcolonies (Fig. 3B). Environmental scanning electron microscope analysis of the Fe-bead clumps from 3-day culture incubations revealed formation of a biofilm on the surface of the beads (Fig. 3C, middle panel) compared with the surface of control Fe-beads incubated in the absence of bacteria (Fig. 3C, top panel). Cells embedded in an organic matrix having an unknown composition were ob-

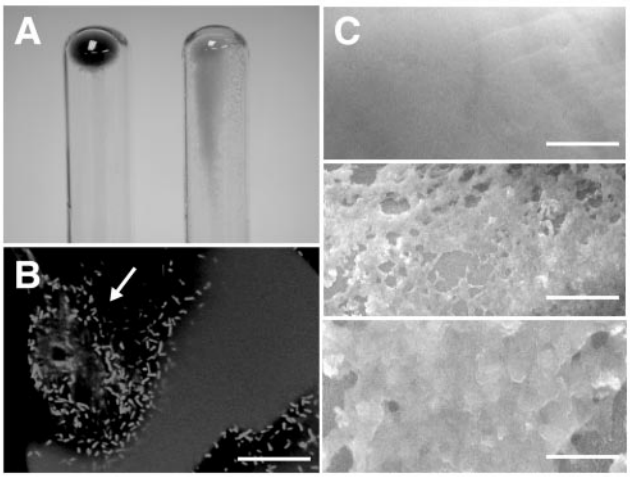

FIG. 3. Biofilm formation on Fe-beads by *S. oneidensis* MR-1. (A) Inverted tubes showing clumping of inoculated Fe-beads after 24 h of incubation (left tube) and an uninoculated control (right tube). (B) Confocal microscopy image of an MR-1 microcolony on an Fe-bead surface after 3 days. Scale bar = 10 μm. The arrow indicates a microcolony. (C) Environmental scanning electron microscopy images of MR-1 biofilms on the Fe-bead surface. (Top panel) Fe-bead surface in the absence of bacteria; (middle panel) Fe-bead surface after 3 days of incubation with MR-1 cells (scale bar = 20 μm); (bottom panel) close-up of Fe-bead surface after 3 days of incubation with MR-1 cells (scale bar = 2 μm).

served in these samples at a higher magnification (Fig. 3C, bottom panel).

Effect of preincubation conditions and cell density on Fe-bead reduction. We initially determined the ability of MR-1 to reduce Fe-beads following anaerobic preincubation in the presence of 1 mM ferric citrate, reasoning that cells actively reducing iron might be more likely to produce a mediator necessary for iron reduction at a distance. *S. algae* BrY was shown previously to reduce iron at a distance in alginate beads when it was grown with ferric citrate as an electron acceptor (47). MR-1 under these conditions reduced more than 80% of the iron in the Fe-beads within 3 days. To test whether anaerobic preincubation under iron-reducing conditions or any anaerobic preincubation was necessary for MR-1 to reduce iron at a distance in the Fe-bead system, we tested cells preincubated anaerobically with 1 mM fumarate and cells grown under oxygen-limited conditions (Fig. 4A). Cells that were preincubated with fumarate reduced the iron in the Fe-beads better than cells that were preincubated with ferric citrate reduced the iron. In contrast, cells that were grown in the presence of oxygen reduced the iron in the Fe-beads consistently more slowly than cells exposed to either anaerobic preincubation treatment reduced the iron.

These results indicate that iron reduction at a distance by MR-1 does not require previous exposure to iron-reducing conditions and suggested that the ability of MR-1 to reduce the iron in the Fe-beads was probably induced under anaerobic conditions. To test this hypothesis, we grew cells under either highly aerobic conditions or anaerobically with fumarate as the sole electron acceptor and inoculated them onto Fe-beads without additional preincubation. The amount of iron reduced by cells grown under the highly aerobic conditions (i.e., with

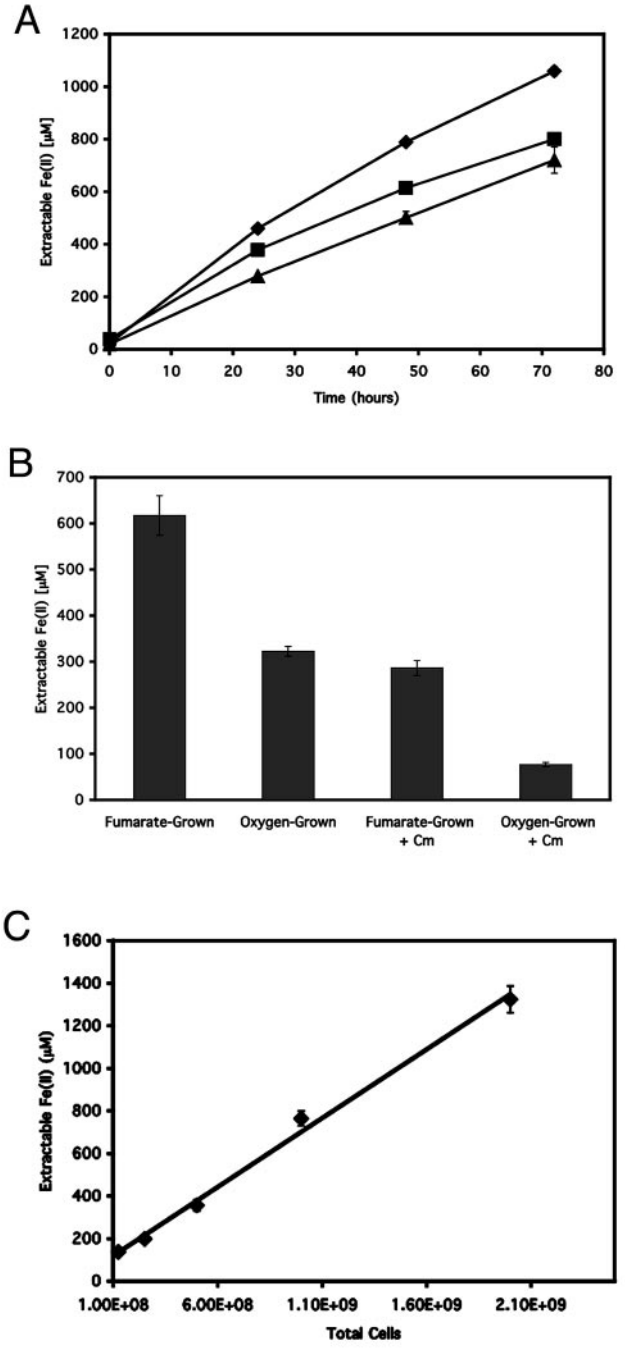

FIG. 4. (A) Reduction of Fe-beads by *S. oneidensis* MR-1 as a function of the preincubation conditions. MR-1 cells were preincubated with 1 mM fumarate (diamonds) or 1 mM ferric citrate (squares) or under oxygen-limited conditions (triangles). (B) Fe-bead reduction by anaerobically and aerobically grown MR-1 cells. Fumarate-grown cells were grown anaerobically with 10 mM fumarate as the electron acceptor, while aerobically grown cells were grown with oxygen as the electron acceptor. Chloramphenicol was added to separate Fe-bead cultures with these cells (+ Cm) to inhibit new protein synthesis. (C) Reduction of Fe-beads as a function of cell density. Serial dilutions of a standard high-density Fe-bead culture inoculum were incubated in separate tubes with Fe-beads. A linear fit to the data is shown. Each data point is the average for duplicate cultures (the error bars indicate the ranges) from 3 days of incubation with the Fe-beads.

TABLE 1. Total protein determined during Fe reduction assays

Form of Fe	Cell density (cells/ml)	Amt of protein (mg/ml) at:		
		0 h	48 h	72 h
Fe-beads	6.7×10^8	0.301 ± 0.010	0.242 ± 0.009	0.186 ± 0.022
	6.7×10^7	0.023 ± 0.001	0.021 ± 0.003	0.015 ± 0.002
Fe(III) (hydr)oxide	6.7×10^8	0.303 ± 0.006	0.270 ± 0.011	0.293 ± 0.021
	6.7×10^7	0.029 ± 0.001	0.029 ± 0.001	0.027 ± 0.001

oxygen as the electron acceptor) was only 50% of the amount of iron reduced by cells grown anaerobically with fumarate as the electron acceptor (Fig. 4B). To determine whether new protein synthesis during anaerobic incubation with the Fe-beads was responsible for the reduction observed, we also performed the experiment in the presence of chloramphenicol. Addition of chloramphenicol to the oxygen-grown cells decreased the amount of iron reduced to the amount observed for formaldehyde-killed cells, while addition of chloramphenicol to the fumarate-grown cells decreased the amount of iron reduced to only 46% of the amount observed for the untreated control (Fig. 4B). Controls in which only ethanol (the solvent for chloramphenicol) was added to cells grown under either condition showed no difference in the reduction rate. This showed that cells grown using oxygen as the electron acceptor are not competent for iron reduction at a distance but can adapt to perform this process during anaerobic incubation in the presence of Fe-beads. Cells grown anaerobically with fumarate as the electron acceptor could reduce iron at a distance in the beads but required continued protein synthesis during incubation to perform maximally. This suggests that either some new component necessary for maximal iron reduction at a distance must be synthesized under these conditions or that some of the components of this process are unstable or degraded during incubation and must therefore be regenerated during experiments.

Because all of these experiments were performed with very high cell densities (6.7×10^8 cells/ml), we examined the relationship between cell density and the ability to reduce iron within the Fe-beads to determine if such high cell densities were required for the process. The amount of iron reduced in the Fe-beads decreased linearly with decreasing cell numbers added in these assays, at least to a cell density of 1×10^8 total cells per assay, while the amount of iron reduced was nonlinear with respect to the higher cell densities at 1×10^7 total cells per assay. At values of $>1 \times 10^8$ total cells per assay the cells still reduced more iron in the Fe-beads over the course of the incubation than was calculated to be present in the outer cortex/surface of the Fe-beads (Fig. 4C). Because these cell densities are high, we considered whether quorum sensing plays a role in controlling the ability of the cells to reduce iron at a distance in the Fe-bead system. The amount of iron reduced for each starting number of cells in 3 days during these experiments remained constant over the range of cell densities examined, suggesting that the cells did not respond to quorum signals.

To determine whether cells grew during these assays, we determined the amounts of total protein extracted from the preparations (Table 1). The amount of total protein stayed constant at a density of 6.7×10^7 cells/ml and decreased by a factor of 2 at the highest cell density (6.7×10^8 cells/ml) over the course of the 3-day incubations with the Fe-beads. For the lowest cell density (6.7×10^6 cells/ml) the protein levels were below the sensitivity of the protein assay and did not increase to a detectable level over the time frame of the experiments (data not shown). Similar results were obtained using Fe(III) (hydr)oxide mineral instead of the Fe-beads as the electron acceptor. This indicates that most cells were not growing during these experiments with either electron acceptor.

Comparison of Fe-bead reduction to free Fe(III) (hydr)oxide particle reduction. Iron reduction rates were compared for Fe-beads and free Fe(III) (hydr)oxide particles using three cell densities (6.7×10^8, 6.7×10^7, and 6.7×10^6 cells/ml) to determine whether there are kinetic differences between Fe-bead reduction and Fe(III) (hydr)oxide reduction. In general, the cells reduced Fe(III) (hydr)oxide particles faster than they reduced the Fe-beads, but regardless of the form of iron, the overall reduction was faster with higher cell densities (Fig. 5A). The rates per cell for the cells reducing the free Fe(III) (hydr)oxide particles were lower for the highest cell density ($3.5 \times 10^{-9} \pm 7.0 \times 10^{-10}$, $1.9 \times 10^{-8} \pm 9.6 \times 10^{-10}$, and $1.1 \times 10^{-8} \pm 8.1 \times 10^{-10}$ μM/h · cell, respectively), while the rates per cell were similar at all cell densities for the cells reducing the Fe-beads ($7.3 \times 10^{-9} \pm 1.0 \times 10^{-9}$, $6.8 \times 10^{-9} \pm 7.7 \times 10^{-10}$, and $5.9 \times 10^{-9} \pm 1.9 \times 10^{-9}$ μM/h · cell, respectively) (Fig. 5B). The lowest cell density incubated with the Fe(III) (hydr)oxide mineral also gave a lower reduction rate than the intermediate cell density. This suggests that there was an optimal ratio of cells to mineral for iron reduction under these conditions.

Tubes containing 6.7×10^6 cells/ml did not exhibit more than 10% reduction of the Fe-beads in 18 days but did exhibit increasing reduction of the iron in the assays over this time. Because up to 13.5% of the iron in the Fe-beads may be available for reduction by direct contact at the surface of the beads, it is not clear whether cells at this density are actually capable of reducing iron at a distance in Fe-beads under these conditions. The continuing reduction of the iron in the Fe-beads was probably not due to a significant increase in cell numbers because the amount of total protein did not increase (Table 1). Further support for this conclusion comes from the observation that the rate of iron reduction over the course of the 18-day incubation was linear, whereas a nonlinear increase in iron reduction over time would be expected for significantly increasing cell numbers because higher beginning cell densities resulted in higher rates of iron reduction over time with Fe-beads. Additionally, the Fe-beads did not clump more tightly over the course of the 18-day incubation when they were inoculated at a low cell density, based on a qualitative assessment of the ease of disruption of the clumps by gentle inversion of the tubes. We observed that the beads clumped more tightly with increased numbers of starting cells in these assays (data not shown). This finding supports the hypothesis that the cells inoculated at a lower density did not form increasing amounts of biofilm over the course of the incubation and were therefore probably not growing.

Diffusion of Fe^{3+} out of the beads. Poorly crystalline Fe(III) (hydr)oxide is almost, but not completely, insoluble. To calculate whether the observed microbial reduction of Fe(III) was due to simple low-level dissolution of Fe(III) (hydr)oxide fol-

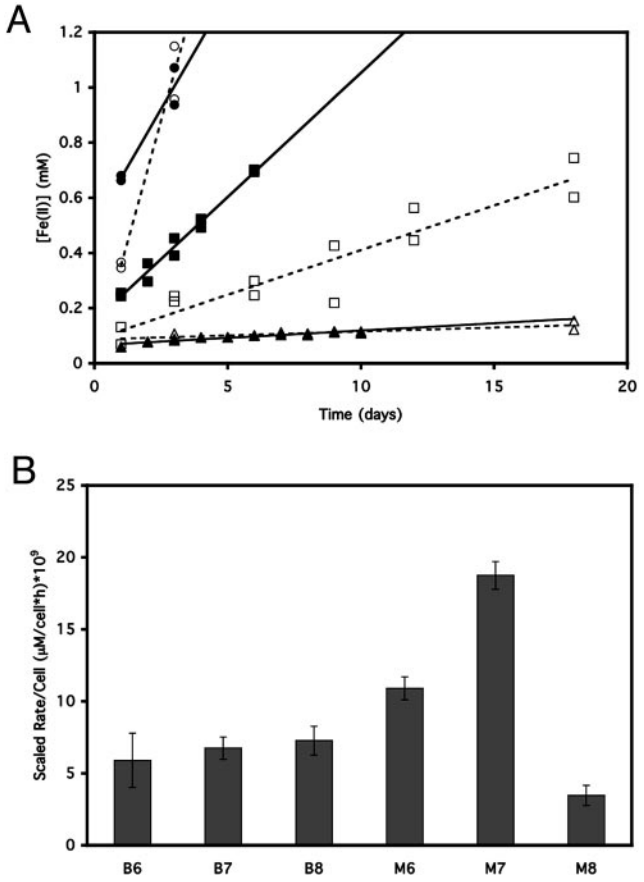

FIG. 5. Fe-bead reduction by *S. oneidensis* MR-1 compared with Fe(III) (hydr)oxide reduction. (A) Time course of iron reduction by 6.7×10^8 (circles), 6.7×10^7 (squares), and 6.7×10^6 (triangles) *S. oneidensis* MR-1 cells/ml with Fe-beads (open symbols and dashed lines) or free Fe(III) (hydr)oxide particles (solid symbols and solid lines) as the electron acceptor. Each data point represents a separate tube sacrificed at a given time for the measurement. Regression lines were calculated by the least-squares method. The initial amount of iron reduced (first day) was not included in the regressions because we could not exclude direct contact reduction of the iron in the bead cortex. (B) Plot of rates per cell calculated from the regressions shown in panel A for different cell densities with Fe-beads or Fe(III) (hydr)oxide. B6, 6.7×10^6 cells/ml with Fe-beads; B7, 6.7×10^7 cells/ml with Fe-beads; B8, 6.7×10^8 cells/ml with Fe-beads; M6, Fe(III) (hydr)oxide with 6.7×10^6 cells/ml; M7, Fe(III) (hydr)oxide with 6.7×10^7 cells/ml; M8, Fe(III) (hydr)oxide with 6.7×10^8 cells/ml. The error bars indicate the standard errors of the slopes of the regression lines.

lowed by diffusion out of the beads and microbial reduction at the bead surface, we estimated the amount of dissolved Fe(III) (i.e., Fe^{3+}) that could diffuse out of the beads under equilibrium conditions.

The flux of Fe^{3+} out of the beads (J_{Fe3+}) could be calculated by $J_{Fe3+} \cong D \times (\Delta C/z)$, where D is the diffusion coefficient for Fe^{3+}, ΔC is the difference between the Fe^{3+} concentration in the beads [controlled by the solubility of Fe(III) (hydr)oxide] and the concentration of Fe^{3+} at the bead surface (operationally defined as zero because of immediate microbial reduction), and z is the distance for diffusion from the center of the beads to the bead surface, given by the bead radius (50 μm). Because the flux of Fe^{3+} out of the beads in an experiment depends on the total bead surface area present, the number of beads per experiment and their surface area must be calculated first.

The number of beads per gram ($\sim 6.6 \times 10^6$ beads per g) could be estimated by dividing the volume per gram of beads (3.45 ml/g, obtained from the bulk bead density given by the supplier, 0.29 g/ml) by the volume per bead (calculated by using an average bead radius of 50 μm). Because the amount of precipitated Fe(III) (hydr)oxide is minor compared to the silica backbone of the beads, we neglected the increase in density due to the Fe(III) (hydr)oxide. The outer surface area per gram of beads (A_{out}) was calculated by multiplying the surface area per bead (assuming an average bead radius of 50 μm) by the number of beads per gram. By dividing A_{out} by the total surface area of the beads (108 m^2/g, as given by the supplier), we calculated that 0.19% of the total surface area was the outer surface of the beads; the remaining 99.81% of the surface area was accounted for by the pore surface inside the beads.

$J_{Fe3+} \cong D \times (\Delta C/z)$ and could be calculated with $D = \sim 1 \times 10^{-5}$ cm^2 s^{-1} (assumed to be similar to the diffusion coefficient for Fe^{2+} given by Sobolev and Roden [58]), $\Delta C = 4 \times 10^{-17}$ mol/liter [derived as described above from the solubility product of $Fe(OH)_3$, $k_{SP} = 4 \times 10^{-38}$ (35)], and $z = 50$ μm to be 2.88×10^{-27} mol/(h · μm^2). In each experiment 0.02 g of beads was present; 0.19% of 108 m^2 (total surface area per gram) yields 4.15×10^{-3} m^2 or 4.15×10^{15} μm^2 for the outer surface area present per experiment, resulting in a flux of 1.19×10^{-11} mol Fe^{3+} per h per experimental setup from the bead interior to the bead surface. Such a flux is several orders of magnitude less than the Fe(III) reduction rates that we observed, and therefore dissolution of Fe(III) (hydr)oxide and diffusion of the dissolved Fe(III) from the bead interior to the bead surface followed by microbial reduction cannot explain our results.

Effects of exogenous electron shuttles and chelators on Fe-bead reduction by MR-1. Because simple equilibrium dissolution and diffusion of Fe^{3+} cannot account for the observed reduction rates, iron reduction at a distance in the Fe-beads by MR-1 must require a diffusible mediator that is either produced by the bacteria during the experiments or present in the medium used for incubation. Such a mediator could be an iron chelator, a redox-active organic molecule (i.e., an electron shuttle), or possibly even the Fe(II) generated by reduction of Fe(III) (hydr)oxides at the bead surface.

The medium used in these experiments contained the synthetic chelator nitrilotriacetic acid (NTA) at a concentration of 78.5 μM as a component of the trace mineral solution, as well as a vitamin solution that could be involved in either iron chelation or electron shuttling. To determine whether these components contributed to iron reduction at a distance by MR-1 with the Fe-beads, we performed experiments in the same medium without adding the vitamin and mineral solutions and observed no differences in the rate of Fe-bead reduction at densities of 6.7×10^7 and 6.7×10^8 cells/ml (data not shown). These results indicate that these components of the media did not serve as significant mediators for Fe-bead reduction by MR-1 under the conditions used in these experiments.

If soluble mediators are produced by the bacteria during

TABLE 2. Fe-bead reduction in the presence of electron shuttles or chelators

Sample assayed	Reduction rate [μM Fe(II)/h]
MR-1[a]	1.23 ± 0.00
MR-1 + 1 μM AQDS	10.86 ± 0.63
MR-1 + 1 μM PMS	1.93 ± 0.09
MR-1 + 2.5 μM PMS	2.08 ± 0.32
MR-1 + 5 μM PMS	2.55 ± 0.20
MR-1 + 10 μM PMS	3.51 ± 0.25
MR-1 + 25 μl/ml anaerobic cell lysate	3.23 ± 0.18
MR-1 + 10 μl/ml anaerobic cell lysate	2.68 ± 0.29
MR-1 + 5 μl/ml anaerobic cell lysate	2.08 ± 0.06
MR-1 + 2.5 μl/ml anaerobic cell lysate	1.41 ± 0.17
MR-1 + 10 μM MK-4	1.13 ± 0.13
MR-1 + 10 μM DHNA	1.20 ± 0.17
MR-1 + 25 μM NTA	1.16 ± 0.03
MR-1 + 25 μM citrate	1.20 ± 0.01
MR-1 + 25 μM Fe(II)	1.17 ± 0.11
MR-1 + 1,000 μM Fe(II)	1.46 ± 0.08

[a] MR-1 reduced 50 μM Fe(III) in the initial 24 h of the experiment.

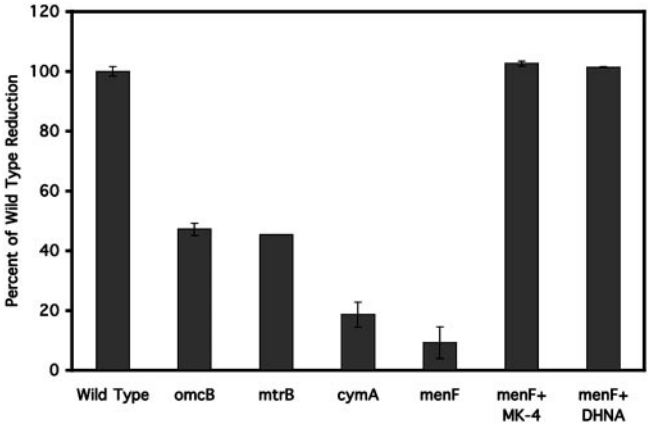

FIG. 6. Reduction of Fe-beads by *S. oneidensis* MR-1 mutants defective in iron reduction. The strains used were strain MR-1 (Wild Type), DKN247 (*omcB*), DKN248 (*mtrB*), DKN249 (*menF*), and DKN250 (*cymA*). *menF* + MK-4, strain DKN249 with 10 μM MK-4 added to the anaerobic preincubation with fumarate; *menF* + DHNA, strain DKN249 with 10 μM DHNA added to the anaerobic preincubation with fumarate. The data indicate the amounts of Fe reduced following our standard 3-day incubation with 6.7×10^8 cells/ml.

Fe-bead reduction and accumulate in the culture fluids, then the addition of "conditioned" supernatants from Fe-bead reducing cultures should increase the rates of iron reduction in freshly inoculated Fe-bead cultures. To facilitate observation of potential increased rates, and because we observed a linear relationship between reduction and cell density down to a density of 1×10^8 cells/ml, the Fe-bead cultures were inoculated with a lower cell density (1×10^8 cells/ml) for the supernatant addition experiments. Similar experiments were used by Nevin and Lovley to demonstrate that soluble mediators allowed iron reduction at a distance in the alginate bead system with strain BrY (45). However, the addition of either reduced or oxidized supernatants from high-cell-density Fe-bead cultures did not stimulate iron reduction at a distance in freshly inoculated Fe-bead cultures. This suggests that a soluble mediator does not accumulate in MR-1 culture supernatants to a level detectable under the assay conditions used.

To ensure that this assay could detect stimulation of Fe-bead reduction by exogenously added mediators and to determine what types of compounds could act as mediators for Fe-bead reduction by MR-1, we performed similar experiments in which we added known artificial electron shuttles and chelators, as well as Fe(II). Fe(II) was added at concentrations from 1 to 25 μM to test the catalytic effects of Fe(II) on the system, as well as at concentrations from 125 to 1,000 μM to test for significant dissolution and mobilization of Fe(III) by the presence of Fe(II). In no experiment did addition of Fe(II) increase the rate of Fe-bead reduction (Table 2), implying that Fe(II) generated from the reduction of surface-available Fe(III) (hydr)oxides was not responsible for accelerating reductive dissolution of the iron from the core of the Fe-beads. However, addition of 1 μM AQDS or ≥1 μM PMS stimulated Fe-bead reduction significantly (Table 2). Addition of 1 μM PMS slightly stimulated Fe-bead reduction, and the stimulation became greater with increasing concentrations of PMS. While these compounds are both redox active and have been shown to stimulate reduction of Fe(III) (hydr)oxide mineral by MR-1 (24), the different concentrations required to obtain similar levels of stimulation of Fe-bead reduction in these assays may reflect differences in the interactions of the compounds with the MR-1 cells.

Addition of 10 μM menaquinone MK-4 or 10 μM DHNA, a biosynthetic precursor of menaquinone, did not stimulate Fe-bead reduction in these assays (Table 2), suggesting that these compounds do not serve as available electron shuttles during Fe-bead reduction by MR-1. Similarly, addition of the strong synthetic iron chelator NTA or the biologically available chelator citrate did not stimulate Fe-bead reduction (Table 2). Because *S. oneidensis* MR-1 has been shown previously to reduce preformed Fe(III)-NTA and ferric citrate (26), these results were not simply due to an inability of the cells to reduce Fe(III) chelated by these compounds in the Fe-bead system and suggested that these chelators were not able to serve as recyclable mediators for Fe-bead reduction under the experimental conditions used. Addition of lysates from aerobic cells to the Fe-bead reduction assays did not stimulate the reduction either (data not shown), although significant stimulation was observed after addition of increasing amounts of cell lysates prepared from the anaerobic cells used to inoculate the bead assays (Table 2). These results suggest that lysis of some of the cells during incubation with the beads may release cellular components that could account for the amount of Fe-bead reduction observed. None of these additions stimulated Fe-bead reduction in the absence of added cells.

Role of the direct contact Fe mineral reduction pathway. To determine whether components of the direct contact pathway defined for Fe(III) (hydr)oxide mineral reduction were involved in iron reduction at a distance, we examined mutants defective in genes involved in the MR-1 mineral reduction pathway (*omcB*, *mtrB*, *cymA*, and *menF* mutants) (Fig. 6). An *omcB* mutant, which was defective in a decaheme cytochrome that is loosely attached to the outer membrane (41), exhibited 45% of the wild-type reduction levels with the Fe-beads. Similar results were observed for an *mtrB* mutant, which was defective in a different outer membrane protein (2, 38) that is

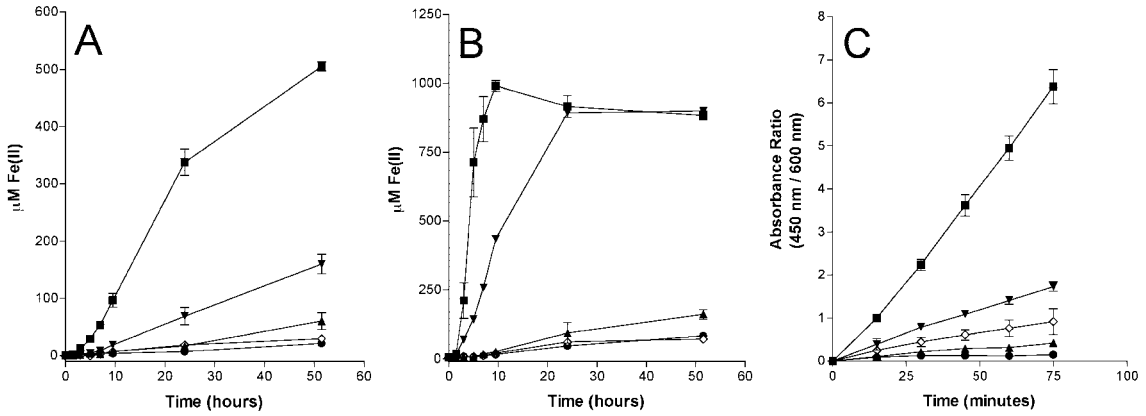

FIG. 7. Reduction of Fe(III) (hydr)oxide, ferric citrate, or AQDS by *S. oneidensis* MR-1 mutants defective in electron transfer. (A) Reduction of 0.5 mM Fe(III) (hydr)oxide; (B) reduction of 1 mM ferric citrate; (C) reduction of 1 mM AQDS. Symbols: ■, wild-type strain MR-1; ▼, *omcB* mutant DKN247; ▲, *mtrB* mutant DKN248; ●, *menF* mutant DKN249; ◇, *cymA* mutant DKN250. The error bars indicate the ranges for duplicate cultures for the iron reduction experiments and the standard deviations for triplicate cultures for the AQDS reduction experiment.

required for localization of outer membrane cytochromes (2, 38). These results indicate that while Fe-bead reduction utilizes the *omcB-mtrB* Fe reduction pathway, there is an alternate pathway for reduction of the iron from the Fe-beads that can contribute significantly to the reduction of the Fe-beads.

On the other hand, both the *cymA* and *menF* mutants were considerably more defective; the *cymA* mutant reduced less than 20% of the iron in the Fe-beads, and the *menF* mutant exhibited only ~10% reduction. CymA is a cytoplasmic membrane-bound periplasmic *c*-type cytochrome required for anaerobic respiratory electron transport (43). Because the *menF* gene encodes a protein in the first committed step in menaquinone biosynthesis, we tested whether the *menF* mutant could be rescued for Fe-bead reduction by addition of exogenous menaquinone to determine whether any intermediates or products of the menaquinone biosynthetic pathway served as mediators during Fe-bead reduction. When provided with exogenous MK-4 or DHNA, the *menF* mutant was completely rescued for Fe-bead reduction (Fig. 6). Because MK-4 itself does not serve as a mediator for Fe-bead reduction (Table 2), this result indicates that MK-4 rescues the electron transport defect of this mutant but that Fe-bead reduction does not require intermediates of the menaquinone biosynthetic pathway.

Given the somewhat surprising result that the *omcB* and *mtrB* mutants still reduced approximately one-half of the iron within the Fe-beads over the 3-day incubation period of the assays, we decided to compare the rates of reduction by these mutants of Fe(III) (hydr)oxide mineral, the soluble chelate ferric citrate, and the soluble artificial electron shuttle AQDS (Fig. 7). Consistent with previous reports (39, 48, 54), menaquinone biosynthesis was required for significant reduction of any of these compounds. CymA was also absolutely required for significant reduction of Fe compounds, as previously described (36), although the extent of AQDS reduction in a *cymA* mutant was not reported previously. However, the abilities of the *omcB* and *mtrB* mutants to reduce the three compounds differed depending on the substrate. As observed previously (2, 3, 38, 42), the *mtrB* mutant was more defective in Fe(III) (hydr)oxide mineral reduction than the *omcB* mutant, but both mutants were considerably defective. On the other hand, the *mtrB* mutant was considerably defective in ferric citrate reduction, whereas the *omcB* mutant was only slightly slower than the wild type. The results for AQDS reduction by these mutants were similar to the results for the Fe(III) (hydr)oxide mineral; both the *omcB* and *mtrB* mutants had a substantial defect, but the *mtrB* mutant was affected more seriously. These results suggest that the electron shuttle AQDS is primarily reduced by the direct contact pathway used for Fe(III) (hydr)oxide mineral reduction involving *omcB*, while the soluble chelate ferric citrate is substantially reduced by an alternate pathway that does not require *omcB*. The residual activity in these mutants argues that in addition to the *omcB*-mediated pathway of Fe reduction, there is an alternate pathway that provides considerable reduction of all of these substrates and requires *mtrB* for its activity. In the absence of *mtrB*, a small fraction of these substrates is still reduced by an unknown mechanism, but this appears to provide only a minor contribution to the reduction of these compounds (Fig. 8). This differs significantly from iron reduction at a distance in the Fe-bead system, in which *mtrB* is not absolutely required for reduction.

DISCUSSION

A key challenge facing researchers investigating microbial mineral reduction is to elucidate the molecular details of the reduction process. This is a particularly difficult task, as it straddles fundamental questions relating to electron transfer in both proteins (18) and minerals (69). Although "direct" and "indirect" mechanisms of microbial mineral reduction are often presented as mechanisms that are different from one another, the extent to which they are different or overlap is unclear. For example, much of the biochemical machinery that is required for iron reduction may be the same regardless of whether bacteria come in direct contact with or are at a distance from the mineral that they are reducing. Accordingly, we set out to develop a system that would enable us to explore how direct and indirect mineral reduction pathways are related

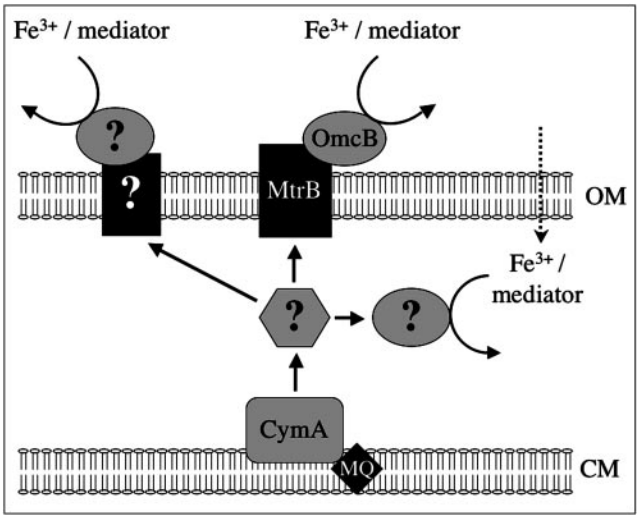

FIG. 8. Model for iron reduction at a distance in *S. oneidensis* MR-1. Chelated Fe(III) or a redox-active mediator is reduced extracellularly by the OmcB-MtrB complex necessary for iron mineral reduction. In the absence of or in addition to this reduction pathway, chelated Fe(III) or the redox-active mediator is reduced by an alternate pathway that may involve other redox-active outer membrane complexes (such as the *mtrDEF* complex or the putative outer membrane molybdopterin oxidoreductase complexes encoded by the SO1427-SO1432 and SO4362-SO4357 gene clusters). Alternatively, chelated Fe(III) or the redox-active mediator may be transported into the bacterial periplasm and reduced by periplasmic electron transport components, such as low-potential multiheme *c*-type cytochromes. OM, outer membrane; MQ, menaquinone; CM, cytoplasmic membrane.

to each other by utilizing *S. oneidensis* strain MR-1 as a model system.

Before we investigated the mechanisms of "direct" and "indirect" iron reduction by *S. oneidensis*, it was necessary to establish whether in fact *S. oneidensis* is capable of catalyzing iron reduction at a distance. Previous studies employing Fe(III) (hydr)oxides sequestered in alginate beads provided evidence which suggested that iron can be reduced at a distance by *Shewanella* and *Geothrix* species (46, 47). In an effort to reproduce these results and to define the conditions under which iron reduction at a distance occurs for *S. oneidensis* strain MR-1, we developed an assay that is similar to the alginate bead method but which makes use of porous glass beads coated on their outer and inner surfaces with Fe(III) (hydr)oxides (Fe-beads). This system has advantages over the alginate bead method in that it is stable at a wide range of pH values and is physically well characterized (e.g., the location of iron is precisely defined, as are the sites of iron release). Our experimental design differed from previous tests with alginate beads in the following additional respects: (i) we did not provide any Fe(III) (hydr)oxides to the cells other than those within the Fe-beads themselves, and (ii) we used much higher cell densities, which resulted in much higher and therefore more easily detectable rates of Fe-bead reduction.

Because our calculations indicated that a maximum of 13.5% of the iron in the Fe-bead system is available for reduction by direct contact, the vast majority of the iron (>86.5%) can be reduced only by an indirect mechanism. Thus, the Fe-beads provide an effective means of assaying for iron reduction at a distance via one or more of three processes: (i) dissolution of Fe(III) from the beads and subsequent microbial reduction of the ferric ion [possibly facilitated by Fe(II)], (ii) mobilization of Fe(III) from the beads to the cells by an Fe(III)-chelator complex, and/or (iii) electron transfer from the cells to the Fe(III) inside the beads by an extracellular electron shuttle. Our data are consistent with the conclusions of Nevin and Lovley (46, 47) for *S. algae* and *G. fermentans* and demonstrate that *S. oneidensis* is capable of reducing iron at a distance using the Fe-bead system. Under the conditions of our assay, MR-1 does not appear to be able to grow, either with the Fe-beads or with an Fe mineral as an electron acceptor.

MR-1 actively catalyzed iron reduction at a distance with the Fe-beads under anaerobic conditions. This was shown by the fact that killed cells exhibited minimal reduction of Fe-glass beads and by the fact that new protein synthesis was required for both aerobically and anaerobically grown cells to reduce Fe-beads at the maximum rates. Although cells that were pregrown under anaerobic conditions (e.g., with fumarate or ferric citrate as the electron acceptor) prior to a trial in the Fe-bead assay reduced iron at a distance faster than aerobically grown cells, the latter cells could reduce iron at a distance if they were given time to adapt to anaerobic conditions. The fact that anaerobically grown cells still required new protein synthesis to achieve maximal Fe-bead reduction suggests either that some new component(s) necessary for Fe bead reduction must be synthesized under these conditions or that some of the components are degraded and/or lose their activity and must therefore be regenerated during the assay. Such components may include functions necessary for attachment of the cells to the Fe-beads and subsequent biofilm formation or may involve components of the anaerobic electron transport chain that are missing in aerobic cells and are expressed only when the cells are allowed to adapt to anaerobic conditions.

Interestingly, iron reduction in the Fe-bead system did not appear to be limited by the availability of Fe(III) reduction sites at high cell densities, in contrast to previous findings that the rates of ferric mineral reduction by *S. algae* BrY and *Shewanella* sp. strain MR-4 reached a plateau at high cell densities (13, 52). In the case of ferric minerals, this plateau was attributed to saturation of the reduction sites on the mineral surface. In our comparative experiments with minerals and Fe-beads, the rate per initial cell number decreased at higher cell densities in the presence of Fe(III) (hydr)oxides, as previously observed (13, 52), but the rates of Fe-bead reduction per cell were similar for all cell densities. Although most of the iron in the bead system is inside the pores and therefore further from the cells, unlike the case for iron minerals, any given iron atom in the Fe-beads is likely to be reactive in this matrix because it is exposed to the water interface and therefore accessible for diffusion, chelation, and/or reduction. This suggests that surface saturation is not limiting in the Fe-bead system and that the rate-limiting step is most likely diffusion.

Assuming that iron reduction in the Fe-bead system is diffusion controlled, the next question is, controlled by diffusion of what? Based on our calculations, dissolution of the Fe(III) (hydr)oxides to release ferric ion cannot account for the rates of iron reduction observed in our experiments. Therefore, the diffusible molecule must represent a mediator of some sort,

either an iron-chelate complex, an electron shuttle, or ferrous ion produced by reduction of surface Fe(III) (hydr)oxides on the Fe-beads. The fact that addition of exogenous Fe(II) to our bead assays did not stimulate reduction of the Fe(III) within the Fe-beads rules out the possibility of a significant role for Fe(II) as a mediator of dissolution of the Fe(III) (hydr)oxides present within the Fe-beads.

At this point it is still not clear what mediates iron reduction at a distance in our system. Our data show that iron is depleted inside the beads. We do not know whether the iron leaves as Fe(III), presumably with the aid of chelators, or as dissolved Fe(II) after it is reduced inside the pores. We did not observe detectable concentrations of dissolved Fe(III) in the Fe-bead system (in contrast to what was reported previously for *S. algae* BrY in the presence of alginate beads [47]), as would be expected if a chelator were present at significant levels. Moreover, we could not find evidence in spent supernatants from Fe-bead cultures for any other factor (e.g., an electron shuttle) that stimulates iron reduction at a distance under the conditions of our experiments. Microscopic examination of the Fe-beads revealed that MR-1 colonizes their surfaces, forming a matrix with characteristic microcolonies. On a macroscopic scale, biofilm formation is obvious in tubes inoculated with the Fe-beads and cells due to establishment of a compact aggregate that readily reforms after physical disruption. The extracellular matrix of the biofilms likely creates a suitable environment for the trapping and cycling of mediators that catalyze iron reduction at a distance, thus explaining our inability to detect Fe chelators and/or electron shuttles in the Fe-bead culture supernatants. This environment could also concentrate such a mediator at the Fe(III) (hydr)oxide surface coated by the biofilm matrix and might therefore promote more efficient iron reduction than a freely soluble mediator.

Notably, addition of the synthetic chelator NTA did not increase the rate of Fe-bead reduction, whereas addition of different electron shuttles (i.e., AQDS or phenazines) did. With the caveat that these synthetic mediators may not be comparable to the native mediator, at this time we favor the interpretation that MR-1 uses an electron shuttle to reduce iron at a distance but that it acts locally within the biofilm-bead environment. Whether this shuttle is specific or derived from a more general pool of redox-active molecules present within the cells that are released as the cells lyse remains to be determined. Because appreciable lysis is known to occur in biofilms (4, 68), it seems reasonable to speculate that mediators of iron reduction in natural systems may include molecules from this pool. The fact that menaquinone rescued reduction of the Fe-beads by a *menF* mutant of MR-1 but did not stimulate Fe-bead reduction by wild-type cells demonstrated that the mediator used for iron reduction at a distance is not a product of the menaquinone biosynthetic pathway. This rules out the previously described quinone-like molecule derived from the menaquinone pathway (48, 67) as an electron shuttle for iron reduction at a distance.

Interestingly, regulation of the production of some biologically produced mediator compounds in other organisms (e.g., phenazine electron shuttles produced by pseudomonads) is controlled by low oxygen tension, as well as by high cell density using acyl-homoserine lactone signaling involving homologs of the LuxI and LuxR proteins (9, 65). In the case of MR-1, however, the genes controlling the biosynthesis of the mediator do not appear to be regulated by quorum sensing. Two facts support this: (i) the rate of Fe-bead reduction per cell appears to be independent of cell density, and (ii) the addition of spent culture fluids from high-cell-density cultures to lower-density cultures does not stimulate Fe-bead reduction. Consistent with this, *S. oneidensis* does not have homologs of the *luxI* or *luxR* genes in its genome (which enable the production of and response to acyl homoserine lactone signaling molecules), although it does possess a homolog of *luxS* (ORF SO1101). In other bacteria, LuxS is necessary for the synthesis of furanosyl-based quorum signals (56), but we have no reason to believe that such signals regulate the expression of genes required for Fe-bead reduction.

Not surprisingly, the Fe reduction in the Fe-bead system appears to use many of the proteins and electron carriers that are involved in reduction of soluble or particulate iron, including at least menaquinone, CymA, MtrB, and OmcB. Because the outer membrane of MR-1 is the first bacterial component that a mediator compound would encounter in cycling between the cell and the mineral surface, it makes sense that electron carriers designed to transfer electrons from the bacterial cytoplasmic membrane to the outer membrane would also be used to reduce an extracellular mediator of iron reduction at a distance. *omcB* and *mtrB* mutants are defective (but not completely eliminated) in reducing iron at a distance with the Fe-beads relative to wild-type MR-1, as has been observed for these mutants in experiments done with Fe(III) (hydr)oxide particles (2, 3, 38, 42). However, the *mtrB* mutants are much more defective for Fe(III) (hydr)oxide particle reduction compared to wild-type MR-1 than they are for Fe-bead reduction. This indicates that even though "direct" and "indirect" pathways of iron reduction both can utilize the outer membrane Fe reduction pathway, the mediator for iron reduction at a distance can use alternate pathways not available for direct contact-mediated iron reduction. Such pathways may include transport of the mediator to the periplasm and reduction of the mediator there by electron carriers, such as the many periplasmic multiheme cytochromes present in MR-1 (33).

Alternatively, other redox-active complexes potentially present on the surface of MR-1 may also be involved in reduction of the mediator outside the cell. There are several other examples of gene clusters in the MR-1 genome that, like the *omcAB-mtrAB* gene cluster, encode predicted redox-active lipoproteins, periplasmic multiheme *c*-type cytochromes, and integral outer membrane proteins. One of these clusters contains the *mtrDEF* genes (ORFs SO1782 to SO1780) upstream of the *omcAB-mtrAB* gene cluster, while two other clusters contain genes encoding redox-active lipoproteins closely related to dimethyl sulfoxide reductases (ORFs SO1427 to SO1432 and ORFs SO4362 to SO4357). Protein localization prediction programs indicate that these redox-active lipoproteins may be localized to the MR-1 outer membrane, as are the OmcA and OmcB lipoproteins. While many of these proteins contain obvious electron transport protein motifs, their role might also include facilitating interactions with the Fe-bead surface. These potential pathways for iron reduction at a distance are summarized in the model shown in Fig. 8.

Recently, it has been suggested (36) that "indirect" iron reduction by *S. oneidensis* MR-1 should not be likely to occur

given the strong evidence for "direct" reduction involving contact with the iron minerals. However, the presence of direct contact-driven reduction does not necessarily exclude the possibility of indirect mediator-driven reduction, and both processes might occur under the same conditions. Moreover, in light of our data that "direct" and "indirect" iron reduction pathways utilize the MtrB/OmcB reduction system, more information at a highly resolved biochemical level is necessary to determine how this system reduces substrates. How close must a multiheme outer membrane protein such as OmcB come to Fe particles to reduce them directly? In a study of chromium(VI) reduction to chromium(III) by cytochrome c_7 (a multiheme cytochrome) from *Desulfuromonas acetoxidans*, it was found that the chromate ion (CrO_4^{2-}) is located ~8 Å from the iron of the heme that is thought to be the electron donor to CrO_4^{2-} (1). In the case of *S. oneidensis* (or any other iron-reducing bacterium, for that matter), we have yet to solve the solid-state structure of OmcB (or a functionally equivalent protein) and to determine the binding site of the terminal electron acceptor (e.g., ferric iron in some form or an electron shuttle that is cycled between the oxide and the enzyme) relative to the terminal heme donor of the protein. At present, we do not have enough structural data to make a case for or against "direct" contact-mediated reduction under most circumstances, but we can constrain the problem theoretically.

To date, the greatest distance that has been measured for any natural electron transfer reaction is ~20 Å (i.e., 2 nm), the length of the electron tunneling pathway from Cu_A to heme *a* in cytochrome *c* oxidase (50, 62). This distance comes close to what is theoretically believed to be the limit for a single nonadiabatic electron transfer event (18). For electron transfer between a multiheme cytochrome on the outer membrane of a cell and a mineral surface to be "direct," presumably this distance must be on the order of 2 nm or less. Given that ferric oxide nanoparticles have been shown to adsorb to the surface of *S. putrefaciens* strain CN-32 and in some instances even penetrate the outer membrane and peptidoglycan layers (16), it is reasonable to speculate that multiheme cytochromes present in the outer membrane of *Shewanella* spp. might come close enough to the ferric oxide surface for electron transfer to occur to a surface-associated iron atom. However, in contexts where cells do not come close enough to ferric oxide particles for direct binding of surface-associated Fe(III), a mediator compound (e.g., an iron chelator or an electron shuttle) appears to be necessary (25). Biofilms, such as those found in association with corroding oil pipelines (15) or fuel cell electrodes (6, 7), provide such a context, and it is striking that the conditions under which iron reduction at a distance is optimal are the same as the conditions that describe a biofilm environment (e.g., high cell density, low oxygen tension).

ACKNOWLEDGMENTS

Grant support from the Office of Naval Research, the Luce Foundation, and the Packard Foundation to D.K.N. is gratefully acknowledged. A.K. received support from the DFG.

We thank Manisha Lotlikar and the 2003 International Geobiology class for technical assistance; Scott Fendorf, Kevin Rosso, Javier Gonzalez, and members of the Newman lab for helpful discussions; and Kristina Straub and three anonymous reviewers for critical comments that improved the manuscript.

REFERENCES

1. **Assfalg, M., I. Bertini, M. Bruschi, C. Michel, and P. Turano.** 2002. The metal reductase activity of some multiheme cytochromes *c*: NMR structural characterization of the reduction of chromium(VI) to chromium(III) by cytochrome c7. Proc. Natl. Acad. Sci. USA **99:**9750–9754.
2. **Beliaev, A. S., and D. A. Saffarini.** 1998. *Shewanella putrefaciens mtrB* encodes an outer membrane protein required for Fe(III) and Mn(IV) reduction. J. Bacteriol. **180:**6292–6297.
3. **Beliaev, A. S., D. A. Saffarini, J. L. McLaughlin, and D. Hunnicutt.** 2001. MtrC, an outer membrane decahaem c cytochrome required for metal reduction in *Shewanella putrefaciens* MR-1. Mol. Microbiol. **39:**722–730.
4. **Beveridge, T. J., S. A. Makin, J. L. Kadurugamuwa, and Z. S. Li.** 1997. Interactions between biofilms and the environment. FEMS Microbiol. Rev. **20:**291–303.
5. **Blattner, F. R., G. Plunkett, C. A. Bloch, N. T. Perna, V. Burland, M. Riley, J. ColladoVides, J. D. Glasner, C. K. Rode, G. F. Mayhew, J. Gregor, N. W. Davis, H. A. Kirkpatrick, M. A. Goeden, D. J. Rose, B. Mau, and Y. Shao.** 1997. The complete genome sequence of *Escherichia coli* K-12. Science **277:**1453–1474.
6. **Bond, D. R., D. E. Holmes, L. M. Tender, and D. R. Lovley.** 2002. Electrode-reducing microorganisms that harvest energy from marine sediments. Science **295:**483–485.
7. **Bond, D. R., and D. R. Lovley.** 2003. Electricity production by *Geobacter sulfurreducens* attached to electrodes. Appl. Environ. Microbiol. **69:**1548–1555.
8. **Caccavo, F., R. P. Blakemore, and D. R. Lovley.** 1992. A hydrogen-oxidizing, Fe(III)-reducing microorganism from the Great Bay Estuary, New Hampshire. Appl. Environ. Microbiol. **58:**3211–3216.
9. **Chin-A-Woeng, T. F. C., D. van den Broek, G. de Voer, K. van der Drift, S. Tuinman, J. E. Thomas-Oates, B. J. J. Lugtenberg, and G. V. Bloemberg.** 2001. Phenazine-1-carboxamide production in the biocontrol strain *Pseudomonas chlororaphis* PCL1391 is regulated by multiple factors secreted into the growth medium. Mol. Plant-Microbe Interact. **14:**969–979.
10. **Coates, J. D., D. J. Ellis, C. V. Gaw, and D. R. Lovley.** 1999. *Geothrix fermentans* gen. nov., sp. nov., a novel Fe(III)-reducing bacterium from a hydrocarbon-contaminated aquifer. Int. J. Syst. Bacteriol. **49:**1615–1622.
11. **Coates, J. D., E. J. P. Phillips, D. J. Lonergan, H. Jenter, and D. R. Lovley.** 1996. Isolation of *Geobacter* species from diverse sedimentary environments. Appl. Environ. Microbiol. **62:**1531–1536.
12. **Croal, L., J. A. Gralnick, D. Malasarn, and D. K. Newman.** 2004. The genetics of geochemistry. Annu. Rev. Genet. **38:**175–202.
13. **Dollhopf, M. E., K. H. Nealson, D. M. Simon, and G. W. Luther.** 2000. Kinetics of Fe(III) and Mn(IV) reduction by the Black Sea strain of *Shewanella putrefaciens* using in situ solid state voltammetric Au/Hg electrodes. Mar. Chem. **70:**171–180.
14. **Dubiel, M., C. H. Hsu, C. C. Chien, F. Mansfeld, and D. K. Newman.** 2002. Microbial iron respiration can protect steel from corrosion. Appl. Environ. Microbiol. **68:**1440–1445.
15. **Flemming, H. C.** 1993. Biofilms and environmental protection. Water Sci. Technol. **27:**1–10.
16. **Glasauer, S., S. Langley, and T. J. Beveridge.** 2001. Sorption of Fe (hydr)oxides to the surface of *Shewanella putrefaciens*: cell-bound fine-grained minerals are not always formed de novo. Appl. Environ. Microbiol. **67:**5544–5550.
17. **Glasauer, S., P. G. Weidler, S. Langley, and T. J. Beveridge.** 2003. Controls on Fe reduction and mineral formation by a subsurface bacterium. Geochim. Cosmochim. Acta **67:**1277–1288.
18. **Gray, H. B., and J. R. Winkler.** 1996. Electron transfer in proteins. Annu. Rev. Biochem. **65:**537–561.
19. **Haas, J. R., and T. J. Dichristina.** 2002. Effects of Fe(III) chemical speciation on dissimilatory Fe(III) reduction by *Shewanella putrefaciens*. Environ. Sci. Technol. **36:**373–380.
20. **Hansel, C. M., S. G. Benner, J. Neiss, A. Dohnalkova, R. K. Kukkadapu, and S. Fendorf.** 2003. Secondary mineralization pathways induced by dissimilatory iron reduction of ferrihydrite under advective flow. Geochim. Cosmochim. Acta **67:**2977–2992.
21. **Hansel, C. M., S. G. Benner, P. Nico, and S. Fendorf.** 2004. Structural constraints of ferric (hydr)oxides on dissimilatory iron reduction and the fate of Fe(II). Geochim. Cosmochim. Acta **68:**3217–3229.
22. **Heidelberg, J. F., I. T. Paulsen, K. E. Nelson, E. J. Gaidos, W. C. Nelson, T. D. Read, J. A. Eisen, R. Seshadri, N. Ward, B. Methe, R. A. Clayton, T. Meyer, A. Tsapin, J. Scott, M. Beanan, L. Brinkac, S. Daugherty, R. T. DeBoy, R. J. Dodson, A. S. Durkin, D. H. Haft, J. F. Kolonay, R. Madupu, J. D. Peterson, L. A. Umayam, O. White, A. M. Wolf, J. Vamathevan, J. Weidman, M. Impraim, K. Lee, K. Berry, C. Lee, J. Mueller, H. Khouri, J. Gill, T. R. Utterback, L. A. McDonald, T. V. Feldblyum, H. O. Smith, J. C. Venter, K. H. Nealson, and C. M. Fraser.** 2002. Genome sequence of the dissimilatory metal ion-reducing bacterium *Shewanella oneidensis*. Nat. Biotechnol. **20:**1118–1123.
23. **Hernandez, M. E.** 2004. Ph.D. thesis. California Institute of Technology, Pasadena.

24. **Hernandez, M. E., A. Kappler, and D. K. Newman.** 2004. Phenazines and other redox-active antibiotics promote microbial mineral reduction. Appl. Environ. Microbiol. **70:**921–928.
25. **Hernandez, M. E., and D. K. Newman.** 2001. Extracellular electron transfer. Cell. Mol. Life Sci. **58:**1562–1571.
26. **Liu, C. X., Y. A. Gorby, J. M. Zachara, J. K. Fredrickson, and C. F. Brown.** 2002. Reduction kinetics of Fe(III), Co(III), U(VI) Cr(VI) and Tc(VII) in cultures of dissimilatory metal-reducing bacteria. Biotechnol. Bioeng. **80:** 637–649.
27. **Lloyd, J. R., D. R. Lovley, and L. E. Macaskie.** 2003. Biotechnological application of metal-reducing microorganisms. Adv. Appl. Microbiol. **53:**85–128.
28. **Lonergan, D. J., H. L. Jenter, J. D. Coates, E. J. P. Phillips, T. M. Schmidt, and D. R. Lovley.** 1996. Phylogenetic analysis of dissimilatory Fe(III)-reducing bacteria. J. Bacteriol. **178:**2402–2408.
29. **Lovley, D. R.** 1991. Dissimilatory Fe(III) and Mn(IV) reduction. Microbiol. Rev. **55:**259–287.
30. **Lovley, D. R., and E. J. P. Phillips.** 1988. Novel mode of microbial energy metabolism: organic carbon oxidation coupled to dissimilatory reduction of iron and manganese. Appl. Environ. Microbiol. **54:**1472–1480.
31. **Lovley, D. R., and E. J. P. Phillips.** 1987. Rapid assay for microbially reducible ferric iron in aquatic sediments. Appl. Environ. Microbiol. **53:**1536–1540.
32. **Methe, B. A., K. E. Nelson, J. A. Eisen, I. T. Paulsen, W. Nelson, J. F. Heidelberg, D. Wu, M. Wu, N. Ward, M. J. Beanan, R. J. Dodson, R. Madupu, L. M. Brinkac, S. C. Daugherty, R. T. DeBoy, A. S. Durkin, M. Gwinn, J. F. Kolonay, S. A. Sullivan, D. H. Haft, J. Selengut, T. M. Davidsen, N. Zafar, O. White, B. Tran, C. Romero, H. A. Forberger, J. Weidman, H. Khouri, T. V. Feldblyum, T. R. Utterback, S. E. Van Aken, D. R. Lovley, and C. M. Fraser.** 2003. Genome of *Geobacter sulfurreducens*: metal reduction in subsurface environments. Science **302:**1967–1969.
33. **Meyer, T. E., A. I. Tsapin, I. Vandenberghe, L. De Smet, D. Frishman, K. H. Nealson, M. A. Cusanovich, and J. J. Van Beeumen.** 2004. Identification of 42 possible cytochrome c genes in the *Shewanella oneidensis* genome and characterization of six soluble cytochromes. OMICS J. Integr. Biol. **8:**57–77.
34. **Miller, J. H.** 1972. Experiments in molecular genetics. Cold Spring Harbor Laboratory, Cold Spring Harbor, N.Y.
35. **Morel, F. M. M., and J. G. Hering.** 1993. Principles and applications of aquatic chemistry. John Wiley and Sons, Inc., New York, N.Y.
36. **Myers, C. R., and J. A. Myers.** 2004. *Shewanella oneidensis* MR-1 restores menaquinone synthesis to a menaquinone-negative mutant. Appl. Environ. Microbiol. **70:**5415–5425.
37. **Myers, C. R., and J. M. Myers.** 1994. Ferric iron reduction-linked growth yields of *Shewanella putrefaciens* MR-1. J. Appl. Bacteriol. **76:**254–258.
38. **Myers, C. R., and J. M. Myers.** 2002. MtrB is required for proper incorporation of the cytochromes OmcA and OmcB into the outer membrane of *Shewanella putrefaciens* MR-1. Appl. Environ. Microbiol. **68:**5585–5594.
39. **Myers, C. R., and J. M. Myers.** 1993. Role of menaquinone in the reduction of fumarate, nitrate, iron(III) and manganese(IV) by *Shewanella putrefaciens* MR-1. FEMS Microbiol. Lett. **114:**215–222.
40. **Myers, C. R., and K. H. Nealson.** 1988. Bacterial manganese reduction and growth with manganese oxide as the sole electron acceptor. Science **240:** 1319–1320.
41. **Myers, J. M., and C. R. Myers.** 2002. Genetic complementation of an outer membrane cytochrome *omcB* mutant of *Shewanella putrefaciens* MR-1 requires *omcB* plus downstream DNA. Appl. Environ. Microbiol. **68:**2781–2793.
42. **Myers, J. M., and C. R. Myers.** 2001. Role for outer membrane cytochromes OmcA and OmcB of *Shewanella putrefaciens* MR-1 in reduction of manganese dioxide. Appl. Environ. Microbiol. **67:**260–269.
43. **Myers, J. M., and C. R. Myers.** 2000. Role of the tetraheme cytochrome CymA in anaerobic electron transport in cells of *Shewanella putrefaciens* MR-1 with normal levels of menaquinone. J. Bacteriol. **182:**67–75.
44. **Nealson, K. H., and D. Saffarini.** 1994. Iron and manganese in anaerobic respiration—environmental significance, physiology, and regulation. Annu. Rev. Microbiol. **48:**311–343.
45. **Nevin, K. P., and D. R. Lovley.** 2000. Lack of production of electron-shuttling compounds or solubilization of Fe(III) during reduction of insoluble Fe(III) oxide by *Geobacter metallireducens*. Appl. Environ. Microbiol. **66:**2248–2251.
46. **Nevin, K. P., and D. R. Lovley.** 2002. Mechanisms for accessing insoluble Fe(III) oxide during dissimilatory Fe(III) reduction by *Geothrix fermentans*. Appl. Environ. Microbiol. **68:**2294–2299.
47. **Nevin, K. P., and D. R. Lovley.** 2002. Mechanisms for Fe(III) oxide reduction in sedimentary environments. Geomicrobiol. J. **19:**141–159.
48. **Newman, D. K., and R. Kolter.** 2000. A role for excreted quinones in extracellular electron transfer. Nature **405:**94–97.
49. **O'Toole, G. A., L. A. Pratt, P. I. Watnick, D. K. Newman, V. B. Weaver, and R. Kolter.** 1999. Genetic approaches to study of biofilms. Biofilms **310:**91–109.
50. **Ramirez, B. E., B. G. Malmstrom, J. R. Winkler, and H. B. Gray.** 1995. The currents of life: the terminal electron-transfer complex of respiration. Proc. Natl. Acad. Sci. USA **92:**11949–11951.
51. **Roden, E. E., and M. M. Urrutia.** 2002. Influence of biogenic Fe(II) on bacterial crystalline Fe(III) oxide reduction. Geomicrobiol. J. **19:**209–251.
52. **Roden, E. E., and J. M. Zachara.** 1996. Microbial reduction of crystalline iron(III) oxides: influence of oxide surface area and potential for cell growth. Environ. Sci. Technol. **30:**1618–1628.
53. **Rosso, K. M., J. M. Zachara, J. K. Fredrickson, Y. A. Gorby, and S. C. Smith.** 2003. Nonlocal bacterial electron transfer to hemtite surfaces. Geochim. Cosmochim. Acta **67:**1081–1087.
54. **Saffarini, D. A., S. L. Blumerman, and K. J. Mansoorabadi.** 2002. Role of menaquinones in Fe(III) reduction by membrane fractions of *Shewanella putrefaciens*. J. Bacteriol. **184:**846–848.
55. **Saltikov, C. W., A. Cifuentes, K. Venkateswaran, and D. K. Newman.** 2003. The *ars* detoxification system is advantageous but not required for As(V) respiration by the genetically tractable *Shewanella* species strain ANA-3. Appl. Environ. Microbiol. **69:**2800–2809.
56. **Schauder, S., K. Shokat, M. G. Surette, and B. L. Bassler.** 2001. The LuxS family of bacterial autoinducers: biosynthesis of a novel quorum-sensing signal molecule. Mol. Microbiol. **41:**463–476.
57. **Shyu, J. B. H., D. P. Lies, and D. K. Newman.** 2002. Protective role of *tolC* in efflux of the electron shuttle anthraquinone-2,6-disulfonate. J. Bacteriol. **184:**1806–1810.
58. **Sobolev, D., and E. E. Roden.** 2001. Suboxic deposition of ferric iron by bacteria in opposing gradients of Fe(II) and oxygen at circumneutral pH. Appl. Environ. Microbiol. **67:**1328–1334.
59. **Stookey, L. L.** 1970. Ferrozine: a new spectrophotometric reagent for iron. Anal. Chem. **42:**779–781.
60. **Straub, K. L., and B. E. E. Buchholz-Cleven.** 2001. *Geobacter bremensis* sp. nov. and *Geobacter pelophilus* sp. nov., two dissimilatory ferric-iron-reducing bacteria. Int. J. Syst. Evol. Microbiol. **51:**1805–1808.
61. **Straub, K. L., and B. Schink.** 2003. Evaluation of electron-shuttling compounds in microbial ferric iron reduction. FEMS Microbiol. Lett. **220:**229–233.
62. **Tsukihara, T., H. Aoyama, E. Yamashita, T. Tomizaki, H. Yamaguchi, K. Shinzawaitoh, R. Hakashima, R. Yaono, and S. Yoshikawa.** 1995. Structures of metal sites of oxidized bovine heart cytochrome-c-oxidase at 2.8 angstrom. Science **269:**1069–1074.
63. **Turick, C. E., F. Caccavo, and L. S. Tisa.** 2003. Electron transfer from *Shewanella algae* BrY to hydrous ferric oxide is mediated by cell-associated melanin. FEMS Microbiol. Lett. **220:**99–104.
64. **Turick, C. E., L. S. Tisa, and F. Caccavo.** 2002. Melanin production and use as a soluble electron shuttle for Fe(III) oxide reduction and as a terminal electron acceptor by *Shewanella algae* BrY. Appl. Environ. Microbiol. **68:** 2436–2444.
65. **Van Rij, E. T., M. Wesselink, T. F. C. Chin-A-Woeng, G. V. Bloemberg, and B. J. J. Lugtenberg.** 2004. Influence of environmental conditions on the production of phenazine-1-carboxamide by *Pseudomonas chlororaphis* PCL1391. Mol. Plant-Microbe Interact. **17:**557–566.
66. **Venkateswaran, K., D. P. Moser, M. E. Dollhopf, D. P. Lies, D. A. Saffarini, B. J. MacGregor, D. B. Ringelberg, D. C. White, M. Nishijima, H. Sano, J. Burghardt, E. Stackebrandt, and K. H. Nealson.** 1999. Polyphasic taxonomy of the genus *Shewanella* and description of *Shewanella oneidensis* sp. nov. Int. J. Syst. Bacteriol. **49:**705–724.
67. **Ward, M. J., Q. S. Fu, K. R. Rhoads, C. H. J. Yeung, A. M. Spormann, and C. S. Criddle.** 2004. A derivative of the menaquinone precursor 1,4-dihydroxy-2-naphthoate is involved in the reductive transformation of carbon tetrachloride by aerobically grown *Shewanella oneidensis* MR-1. Appl. Microbiol. Biotechnol. **63:**571–577.
68. **Werner, E., F. Roe, A. Bugnicourt, M. J. Franklin, A. Heydorn, S. Molin, B. Pitts, and P. S. Stewart.** 2004. Stratified growth in *Pseudomonas aeruginosa* biofilms. Appl. Environ. Microbiol. **70:**6188–6196.
69. **Williams, A. G. B., and M. M. Scherer.** 2004. Spectroscopic evidence for Fe(II)-Fe(III) electron transfer at the iron oxide-water interface. Environ. Sci. Technol. **38:**4782–4790.
70. **Zachara, J. M., J. K. Fredrickson, S. M. Li, D. W. Kennedy, S. C. Smith, and P. L. Gassman.** 1998. Bacterial reduction of crystalline Fe^{3+} oxides in single phase suspensions and subsurface materials. Am. Mineralog. **83:**1426–1443.